Journal of Ocean, Mechanical and Aerospace
-Science and Engineering-, Vol.16

February 20, 2015

Numerical Study on the Fluid Forces of a Rigid Cylinder Covered by Helical Rods with Gap Due to the Variations of Incoming Flow Direction and Pitch at Reynolds Number 1000

Arief Syarifuddin,[a,*] Rudi Walujo Prastianto,[b] and Silvianita,[b]

[a)]*Graduate Program on Marine Technology, Faculty of Marine Technology, Institut Teknologi Sepuluh Nopember, Surabaya, Indonesia*
[b)]*Department of Ocean Engineering, Faculty of Marine Technology, Institut Teknologi Sepuluh Nopember, Surabaya, Indonesia*

*Corresponding author: ariefsyarifuddin05@gmail.com

Paper History

Received: 28-January-2015
Received in revised form: 6-February-2015
Accepted: 18- February -2015

ABSTRACT

Offshore structures such as a jacket platform, risers, conductors, mooring lines, Spars, and pipelines, are subject to severe vibration due to Vortex-induced vibration (VIV). This vibration can lead the structures to fatigue failure. One of a passive suppression device which effectively reduces the VIV is in the form of triple helical rods with gap covered to a cylinder. The present paper specially discusses the influence of incoming flow direction and pitch of helix on the induced fluid forces acting on the cylinder due to addition of helical rods at Reynolds number (Re) of 10^3. The configuration produced best reduction on drag and lift forces in CFD simulation are with 30D length of pitch for the incoming flow direction of 0° and 60°. Reduction on the drag and lift forces for incoming flow directions of 0° and 60° are respectively, 11.34% and 88.32%, and 10.99% and 97.94%.

KEY WORDS: *Vortex Shedding; Helical Rods with Gap, Incoming Flow Direction; Pitch; Fluid Forces.*

NOMENCLATURE

Re	Reynolds Number
U	Fluid Velocity
D	Diameter of Structure
v	Kinematic Viscosity of Fluid
F_L	Lift Force
F_D	Drag Force
C_L	Lift Coefficient
C_D	Drag Coefficient
ρ	Fluid Density
A	Frontal Area of Structure
μ_t	Eddy or Turbulent Viscosity
k	Turbulent Kinetic Energy
ω	Turbulent Frequency
u	Velocity Vector
F_i	Blending Function
P	Production Rate of Turbulence
σ_k, σ_ω	The Turbulent Prandtl Numbers for k and ω
S	Invariant Measure of The Strain Rate
β^*, α	Constants of The SST Model

1.0 INTRODUCTION

An offshore structure is a structure that has many cylindrical components such as risers, conductors, mooring lines, Spars, and pipelines. Each submerged cylindrical component subjected to fluid flow will undergo the phenomenon called Vortex Induced Vibration (VIV). The VIV is a phenomenon in a fluid flow caused by the shedding of vortices behind the structures due to the interactions of fluid and structure. Vortex is a fluid flow which its particles rotate around its central point. The release of this vortex is called vortex shedding, with its tangential and transversal velocity varies with respect to its radius [1]. The schematic process of vortex shedding can be illustrated in Figure 1.

The existance of VIV encouraged an amount of research to investigate how to reduce its impact. Jones and Lamb in 2003 explained that vortex suppressing devices can be divided into

three categories: topographic devices, shrouds, and wake stabilizers [2].

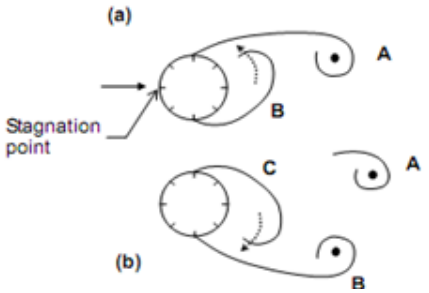

Figure 1: Schematic mechanism of vortex shedding on a cylinder in steady stream [1].

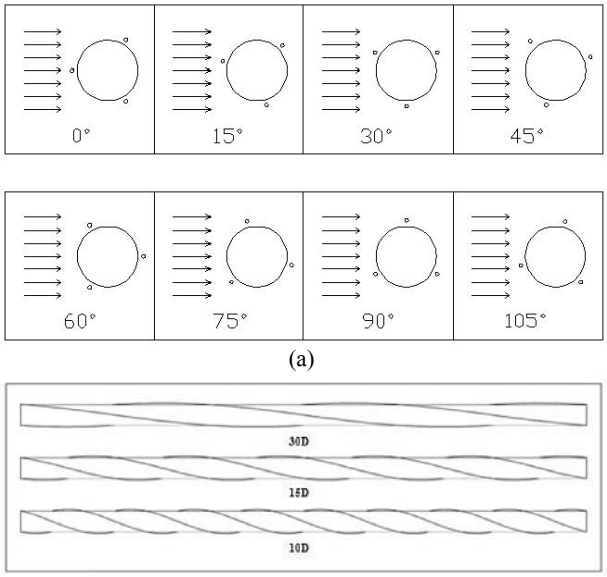

Figure 2: Model of cylinder covered by helical rods with gap (a) the variations of incoming flow direction; (b) the variations of pitch length.

This paper will discuss about the influence of installation of helical rods with gap on a rigid cylinder to the induced drag and lift. Based on previous research that has been done by Sugiwanto, et al. (2013) which explained that the configuration of the model as follows: rods diameter 0.0625D, the length of pitch 15D, and gap 0.0625 m can reduce the drag force by 50% at Re 10^5 [3]. Furthermore, the research which also explained its passive control device has been done by Beu (2013). The best configuration that able to reduce the fluid forces in this research was helical rods with gap installed along 60% of the length of the model and gap 6 mm. It was able to reduce the fluid forces by ±45%. The length of the model used in this research was 4.28 m, and diameter of cylinder was 0.016 m [4]. Experimental study on its passive control device has been done by Arianti (2014) and Prastianto, et. al. (2014). Experiments were carried out in Laboratory of Aero-Gas Dynamics and Vibration (UPT-LAGG), The Agency for the Assessment and Application of Technology (BPPT) in PUSPIPTEK area Serpong using LAGG Mini Wind Tunnel (LMWT). The research which has been done by Arianti (2014) shows that helical rods with gap can reduce the drag force on a cylinder by 47.1% at Re 2.8×10^4, while for the lift force by 43.8% at Re 2.5×10^4 [5]. Whereas, Prastianto, et. al. (2014) shows that the model successfully reduce drag and lift forces respectively by 50% at Re 2.36×10^4 and 25% at Re 2.19×10^4 [6].

This paper specially discusses the influence of variations of the incoming flow direction and the length of pitch on reducing the fluid forces (drag and lift forces) due to installation of helical rods with gap on rigid cylinder at Re = 10^3. Figure 2 shows the variations of the incoming flow direction and pitch. The modeling has been conducted using an Computational Fluids Dynamics (CFD) software known as ANSYS.

2.0 METHOD

2.1 Data Used in this Paper

Some of data used for this paper were obtained from a journal written by Sugiwanto, et al. (2013) [3]. Detail of the data used is presented in Table 1.

Table 1: Cylinder and fluid data [3]

Description	Quantity	Units
Length of cylinder	9.75	m
Diameter of cylinder	0.325	m
Diameter of rods	0.02	m
Gap	0.05	m
Temperature	25	°C
Water density	997	kg/m^3
Dynamic viscosity	8.899x10^{-4}	kg/ms

Determination of the fluid domain for CFD analysis is based on a thesis written by Beu (2013), as shown in Figure 3. The height of fluid domain is adapted from the height of cylinder [4]. The variations used for this paper is presented in Table 2.

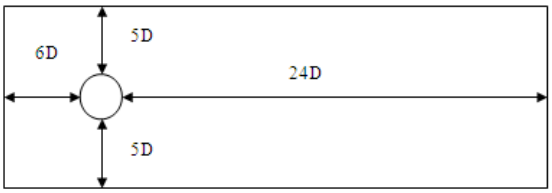

Figure 3: Fluid domain used by the simulation model.

Table 2: Variations used in this paper

Description	Quantity
Length of pitch	30D, 15D, 10D
Incoming flow direction	0°, 15°, 15°, 30°, 45°, 60°, 75°, 90°, and 105°

2.2 Modeling

Initial modeling is done by using 3D CAD for bare cylinder and cylinder covered by helical rods with gap, as shown in Figure 4. The model then be used in CFD software.

(a) (b)

Figure 4: Modeling in 3-D CAD (a) bare cylinder; (b) cylinder covered by helical rods with gap.

2.3 Meshing Sensitivity

Meshing sensitivity is very important in the analysis of CFD software to obtain the appropriate meshing configuration. Meshing sensitivity or it could be called the grid independent is an initial stage in the analysis using CFD software. The model will be discretized its element to obtain a model that approach the real condition. To obtain the appropriate meshing configuration, researchers need to perform some simulations to obtain the point where the value, which in this paper is drag coefficient, begin to converge. The results of some simulations can be seen in Figure 5, but for more details on the information obtained from meshing sensitivity can be seen in Table 3.

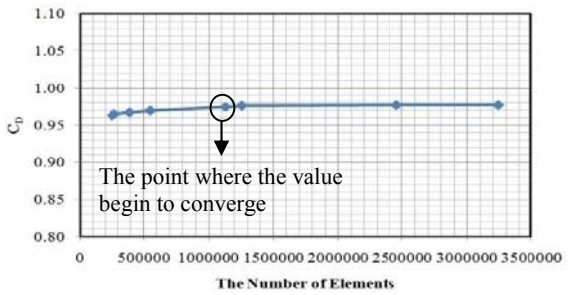

Figure 5: The results of meshing sensitivity analysis.

Table 3: The results of drag coefficient in meshing sensitivity

Simulation	The Number of Elements	F_D (N)	C_D
1	252779	0.0129916	0.9632537
2	272642	0.013008	0.9644696
3	392329	0.0130407	0.9668941
4	549887	0.0130762	0.9695263
5	1128101	0.0131481	0.9748572
6	1254136	0.0131689	0.9763995
7	2454758	0.0131795	0.9771854
8	3239169	0.0131779	0.9770667

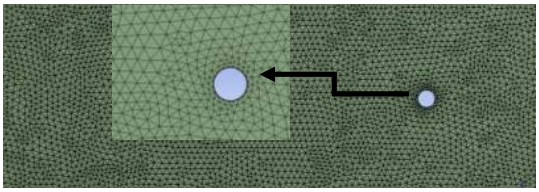

Figure 6: The shape of meshing sensitivity in simulation 5.

Table 3 shows that the value of the C_D begin to converge when simulation 5. Meshing configuration used for the simulation 5 can be seen in Figure 6, while meshing size configuration presented in Table 4. It will be used for all variations in this paper.

Table 4: Meshing size used in this paper

	Value	Unit
Minimum size	0.011125	m
Maximum face size	0.1	m
Max size	0.8225	m
Number of layers	5	
Growth rate	1.2	
Maximum thickness	0.005	m
The shape of meshing in fluid domain	Tetrahedron	
The number of elements	1.128.101	

2.4 Validation of the Model

Validation of the model is done when it has obtained the appropriate meshing configuration. In this paper, model validation performed on drag coefficient of the bare cylinder at Re 10^3. Validation of drag coefficient based on the research conducted by Constantinides, et al. (2006) [7] as presented in Figure 7.

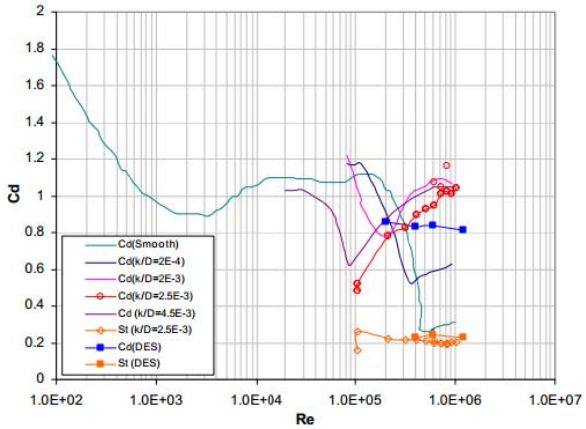

Figure 7: Predicted values of drag coefficient for fixed bare cylinder in CFD simulation and its comparison with experimental data value [7].

Figure 7 shows the comparison between C_D and St. CFD simulation and experimental data for k/D = 0.0025. The red line (circle symbol) and orange line (diamond symbol) are C_D and St. experimental data, whereas the blue and orange lines with box symbols are C_D and St. CFD simulation data. For the other colors are C_D experimental data. Green line is C_D for the smooth cylinder that is used as a reference for validation in this paper.

Some equations are important to consider in the CFD simulation as follows:

- Reynolds number (Re)
  Reynolds number, non-dimensional parameters are well known in the science of fluid mechanics. This name was given in honor of Osborne Reynolds (1842-1916). Engineer from England was who first demonstrated that the combination of variables can be used as standard to

distinguish laminar and turbulent flow. Re is defined as the ratio of inertial forces to viscosity force [8]. Re equation will be used to obtain the fluid velocity of the inlet and the outlet.

$$Re = \frac{UD}{\upsilon} \quad (1)$$

- Turbulent Model SST (Shear Stress Transport)
  Turbulent model used in this paper is SST. SST is a combination of two models of turbulence, namely k-ω and k-ε. SST formulation will replace k-ε behavior in the free stream. So it will avoid the common problem of k-ω models that sensitive for free stream inlet turbulence. SST models has good behavior in negative pressure gradient and flow separation. SST also not produce too much turbulence levels in areas with large normal strains, such as stagnation areas and areas with strong acceleration. The SST formulation according to Menter SST model [9] is:

$$\frac{\partial(\rho k)}{\partial t} + \frac{\partial(\rho u_j k)}{\partial x_j} = P - \beta^* \rho\omega k + \frac{\partial}{\partial x_j}\left[(\mu + \sigma_k \mu_t)\frac{\partial k}{\partial x_j}\right] \quad (2)$$

$$\frac{\partial(\rho\omega)}{\partial t} + \frac{\partial(\rho u_j \omega)}{\partial x_j} = \frac{\gamma}{v_t} P - \beta\rho\omega^2 + \frac{\partial}{\partial x_j}\left[(\mu + \sigma_\omega \mu_t)\frac{\partial \omega}{\partial x_j}\right] + 2(1 - F_1)\frac{\rho\sigma_{\omega 2}}{\omega}\frac{\partial k}{\partial x_j}\frac{\partial \omega}{\partial x_j} \quad (3)$$

and turbulent eddy viscosity is computed from:

$$\mu_t = \frac{\rho a_1 k}{max\,(a_1\omega, SF_2)} \quad (4)$$

- Drag and lift forces
  As a result of changes in the period of vortex shedding, the pressure distribution on the cylinder due to the flow will also change periodically, then it will create periodic variation in the components of the force on the cylinder. The force components are divided into cross flow and in line direction. Component of force in the cross flow direction is called the lift force, while the in line direction called the drag force. Scheme for drag and lift force can be seen in Figure 8. The equation for the drag and lift forces as follow [10]:

$$F_L = \frac{1}{2} C_L \rho A U^2 \quad (5)$$

$$F_D = \frac{1}{2} C_D \rho A U^2 \quad (6)$$

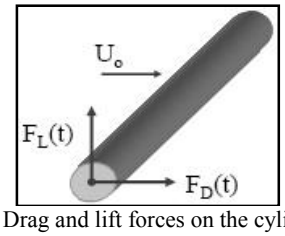

Figure 8: Drag and lift forces on the cylinder [11].

Drag force obtained from CFD simulations using SST turbulence models for bare cylinder at Re 10^3 is 0.01315 N. The drag force converted to drag coefficient by using equation 6. The value of drag coefficient is 0.975. It can be validated by the drag coefficient that obtained from experimental result. The value of drag coefficient that contained from Constantinides, et al. (2006) is 0.968 [7]. The difference between drag coefficient of simulation and experiment is 0.66%. This indicates that the configuration of bare cylinder models used in this simulation are valid.

3.0 RESULT AND DISCUSSION

Having obtained the bare cylinder models were valid, then the next step is to perform a comparison between the fluid forces (drag and lift forces) generated by the bare cylinder and the cylinder covered by helical rods with gap. Several variations of the incoming flow direction and pitch performed on the cylinder covered by helical rods with gap to get the best configuration can reduce the fluid forces.

3.1 Effect Analysis in the Variations of Incoming Flow Direction

As shown in Figure 2 (a), each incoming flow direction will produce different rods configurations. It will be analyzed in the CFD software. The purpose of this analysis is to determine the configuration that generates the greatest reduction of fluid forces. The results obtained from the simulation due to variations of incoming flow direction presented in Table 6.

Table 6: Comparison of C_D and C_L between bare cylinder and cylinder covered by helical rods with gap due to variations of incoming flow direction at Re 10^3

Incoming Flow Direction	Length of Pitch	C_D		C_L	
		Bare	Helix	Bare	Helix
0°	30D	0.97486	0.864	0.00153	0.00018
15°	30D		0.865		0.00067
30°	30D		0.866		0.00568
45°	30D		0.865		0.00337
60°	30D		0.868		0.00003
75°	30D		0.866		0.00853
90°	30D		0.865		0.00298
105°	30D		0.863		0.00220

Table 6 shows the best configuration that generates the greatest reduction of lift force are incoming flow direction of 0° and 60°. Whereas the results of drag force, obtained from simulation, showed little differences that generated in all variations of incoming flow direction. Figure 9 shows the percentage reduction of the fluid forces on the cylinder covered by helical rods with gap.

Figure 9 explains that there is no significant difference in the drag coefficient due to variations of incoming flow direction. The percentage reduction of drag coefficient is between 10.9-11.5%. The incoming flow direction which result the greatest reduction of drag coefficient is 105°, while that result the lowest reduction is 60°. However, it is not enough to conclude that this configuration with incoming flow direction of 105° is the best configuration, because lift coefficient have not been considered in that result. The results obtained for the percentage reduction in the lift coefficient in the variations of incoming flow direction as presented in Figure 10.

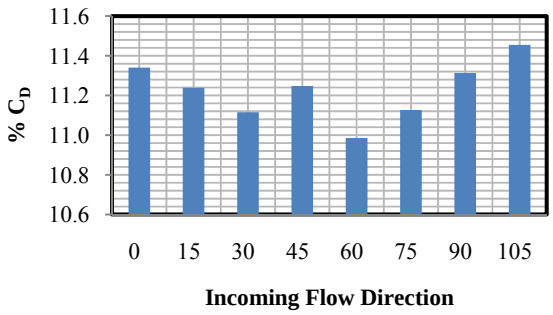

Figure 9: Reducing percentage diagram of the drag coefficient in all variations of incoming flow direction at Re 10^3.

Figure 10 explains that almost all of the rods configuration due to the incoming flow direction on cylinder covered by helical rods with gap increased the lift coefficient (the reducing percentage of lift coefficient is minus) when compared with bare cylinder, except for the configuration of rods due to the incoming flow direction of 0°, 15°, and 60°. The configuration that produce the largest reduction of lift coefficient are the configuration rods due to the incoming flow direction of 0°, 15°, and 60° respectively by 88.32%, 56.32%, and 97.94%. Whereas the reduction of drag coefficient in the configuration rods due to the incoming flow direction of 0°, 15°, and 60° respectively by 11.34%, 11.24%, and 10.99%. It can be concluded that the configuration rods due to the incoming flow direction of 0° and 60° are the greatest reduction of drag and lift forces. The configuration rods due to the incoming flow direction of 0° is the best configuration to reduce drag force, while the configuration rods due to the incoming flow direction of 60° is the best configuration to reduce lift force.

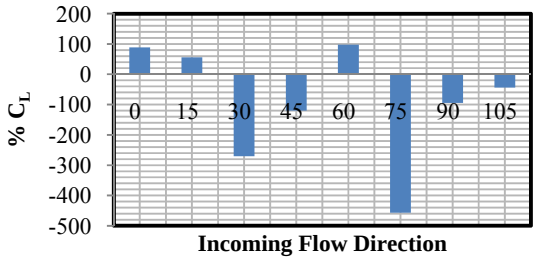

Figure 10: Reducing percentage diagram of the lift coefficient in all variations of incoming flow direction at Re 10^3.

3.2 Effect Analysis in the Variations of Pitch

Previous discussion explains that the configuration rods due to the incoming flow direction of 0° and 60° with length of pitch 30D, and gap 0.05 m (g/D=0.154) is the best configuration to reduce fluid forces. This section will strengthen the previous results that obtained by do variations in the length of pitch. The variations used in this paper are 10D, 15D, and 30D. The results obtained from CFD analysis for the effect of pitch in the fluid forces is presented in Table 7 and Table 8.

Table 7: Comparison of C_D and C_L between bare cylinder and cylinder covered by helical rods with gap due to variations of pitch for incoming flow direction of 0°

Length of Pitch	C_D		C_L	
	Bare	Helix	Bare	Helix
10D	0.97486	0.86565	0.00153	0.00191
15D		0.87252		0.00058
30D		0.86431		0.00018

Table 8: Comparison of C_D and C_L between bare cylinder and cylinder covered by helical rods with gap due to variations of pitch for incoming flow direction of 60°

Length of Pitch	C_D		C_L	
	Bare	Helix	Bare	Helix
10D	0.97486	0.86158	0.00153	0.00031
15D		0.87143		0.00214
30D		0.86776		0.00003

Table 7 shows that for all variations of pitch produce the reduction in the drag force when compared with bare cylinder, the percentage reduction as presented in Figure 11 (a). Whereas for the lift coefficient, just length of pitch 30D which results the reduction of the lift coefficient in both incoming flow direction of 0° and 60°. Length of pitch 10D increase of lift coefficient (the reducing percentage of lift coefficient is minus) in the incoming flow direction of 0°, while the length of pitch 15D increase of lift coefficient in the incoming flow direction of 60°. Percentage reduction in the drag and lift in the variations of pitch for the incoming flow direction of 0° and 60° can be seen in Figure 11.

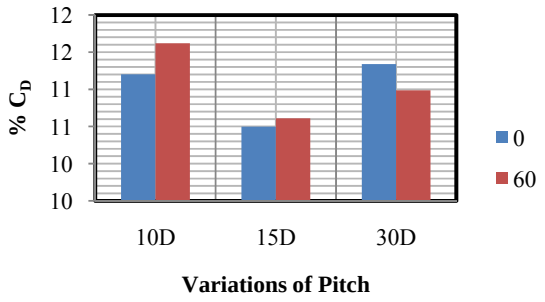

(a)

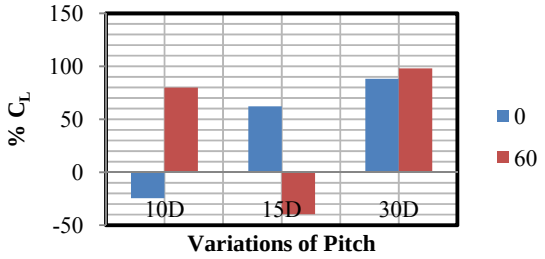

(b)

Figure 11: Variations of pitch for incoming flow direction of 0° and 60° at Re 10^3 (a) Reducing percentage diagram of the drag coefficient; (b) Reducing percentage diagram of the lift coefficient.

From the above explanation, it can be seen that the length of pitch 30D produces the greatest reduction of the fluid forces when compared with the other pitch. The reduction in the length of pitch, it means that the area of cylinder covered by helical rods will be even greater, will lead to increase in the area of the cylinder that will be used in the calculation of force. In this condition, that helical rods would be considered as foreign object that will make area of the cylinder increase. Based on the equation 3, the addition of area that is subject to the flow will increase the fluid forces result.

4.0 CONCLUSION

The configuration of installation helical rods with gap due to incoming flow direction of 0° and 60° with gap 0.05 m (g/D = 0.154) and length of pitch 30D is the best configuration in order to reduce fluid forces at Re 10^3. That configuration produce the greatest reduction of drag and lift forces in incoming flow direction of 0° respectively 11.34% and 88.32%. Beside that incoming flow direction, the greatest reduction of drag and lift forces also occurred in incoming flow direction of 60° respectively 10.99% and 97.94%.

ACKNOWLEDGEMENTS

The first author would like to convey a great appreciation to Directorate of Higher Education (DIKTI) – Ministry of Education and Culture, Republic of Indonesia for the financial support in his study in postgraduate.

REFERENCE

1. Indiyono, P. (1994). *Hidrodinamika Bangunan Lepas Pantai*. SIC, Surabaya, Indonesia.
2. Lubbad, R. K., Loset, S., Gudmestad, O. T., Torum, A. and Moe, G. (2007). Vortex Induced Vibrations of Slender Marine Risers – Effects of Round-Sectioned Helical Strakes, *Proceedings of the 16th International Offshore and Polar Engineering (ISOPE) Conference*, San Francisco, California, USA, May 28 – June 2.
3. Sugiwanto, A., Prastianto, R. W., Murdjito and Djatmiko, E. B. (2013). A Numerical Study on Cylinders with Passive Control Device of Helical Rods with Gap for Reducing Vortex-induced Vibration, *Proceeding of the Second International Conference on Sustainable Infrastructure and Built Environment* (SIBE2013), Proc. Book Vol. III, Institut Teknologi Bandung, Bandung, Indonesia, November 19-20.
4. Beu, M. M. Z. (2013). *Studi Numerik Pengaruh Bentuk Passive Control Device berupa Rods Bergap Berpola Helix terhadap Vortex Induced Vibration (VIV) pada Long Flexible Riser.* Thesis: Program Studi Teknik Perancangan Bangunan Laut, Institut Teknologi Sepuluh Nopember, Surabaya, Indonesia.
5. Arianti, E. (2014). *Studi Eksperimental dan Numerik Pengaruh Penambahan Helical Rod Ber-Gap terhadap Gaya Fluida pada Silinder Rigid Tertumpu Fleksibel.* Thesis: Program Studi Teknik Perancangan Bangunan Laut, Institut Teknologi Sepuluh Nopember, Surabaya, Indonesia.
6. Prastianto, R. W., Musthofa, A. Z. A., Arianti, E., Handayanu, Murdjito, Suntoyo, and Fariduzzaman. (2014). Triple Helical Rods with Gap as A Passive Control Device for Reducing Fluid Forces on A Cylinder, *The 9th International Conference on Marine Technology*, Institut Teknologi Sepuluh Nopember, Surabaya, Indonesia, MT-27, October 24-25.
7. Constantinides, Y., and Oakley O. H. Jr. (2006). Numerical Prediction of Bare and Straked Cylinder VIV, *Procedings of 25th International Conference on Offshore Mechanics and Arctic Engineering*, Hamburg, Germany, June 4-9, pp. 1-9.
8. Munson, B. R., Young, D. F., and Okiishi, T. H. (2002). Fundamentals of Fluid Mechanics, *ISBN 0-471-44250-X*. John Wiley & Sons, Inc., New York, USA.
9. Menter, F. R. (1994). Two-Equation Eddy-Viscosity Turbulence Models for Engineering Applications, *AIAA Journal*, Vol. 32, No. 8, August 1994, pp. 1598-1605. Reston, USA.
10. Cengel, Y. A. and Cimbala, J. M. (2010). *Fluid Mechanics: Fundamentals and Applications.* The McGraw Hill, New York, USA.
11. Purwanti, L. (2008). *Analisa Vortex Induced Vibration Pada Riser Tension Leg Platform*. Bachelor Final Project: Jurusan Teknik Kelautan, Institut Teknologi Sepuluh Nopember, Surabaya, Indonesia.